Indian Journal of Geo-Marine Sciences
Vol. 44(12), December 2015, pp. 1928-1936

# Dynamic Motion Analysis of a Newly Developed Autonomous Underwater Glider with Rectangular and Tapered Wing

Muhammad Yasar Javaid [1], Mark Ovinis[1], Nagarajan Thirumalaiswamy[1], Fakhruldin B M Hashim[1], Adi Maimun[2], Barkat Ullah[1]

[1] Department of Mechanical Engineering,
Universiti Teknologi PETRONAS, Perak, Malaysia
[2] Marine Technology Centre, Faculty of Mechanical Engineering,
Universiti Teknologi Malaysia, Johor Bahru, Malaysia

[E-Mail: yasar248@gmail.com]

*Received 30 October 2015; revised 05 December 2015*

An autonomous underwater glider (AUG) is a self-propelled vehicle whose motion is controlled by shifting its centre of buoyancy and gravity with wings to convert vertical motion into horizontal motion. In this paper, the dynamic motion of a newly developed AUG, including a spiral motion, with rectangular and tapered wing is analysed. The dynamics of the glider, including its hydrodynamic derivatives, is modelled based on the Newton-Euler approach. This model is subsequently used, with a linear quadratic regulator (LQR) control technique, to analyse the glider motion along the sagittal plane, its steady state spiral gliding motion in the vertical plane, and its stability. Results show that the glider has a stable dynamic response and a satisfactory glide performance. Specifically, the external control surface i.e. wings, influence the linear velocity and steady turning radius of glider. Furthermore, it was found that the rectangular winged glider has more dynamic stability because of a higher pitch moment. Additionally, a rectangular winged glider has a smaller spiral turning radius i.e. better manoeuvrability.

[**Keyword:** Underwater glider, Dynamic model, Spiral motion, Dynamic stability]

## Introduction

An autonomous underwater glider (AUG) is a special type of unmanned underwater vehicle that uses buoyancy control, in conjunction with wings to convert vertical motion to horizontal motion, typically in a saw-tooth pattern, to propel itself forward with very low power consumption [1], as shown in (Fig. 1). This is an emerging technology in underwater vehicles due to its high energy efficiency.

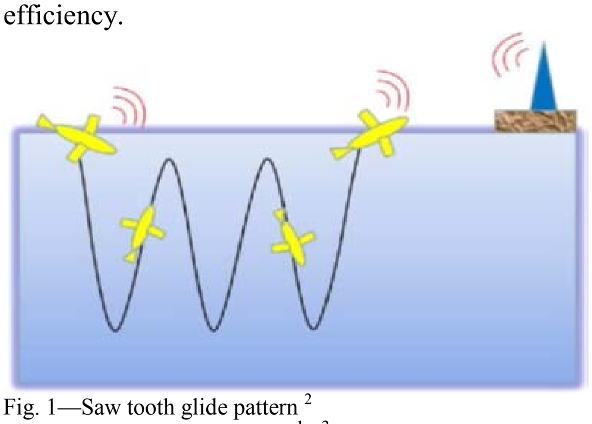

Fig. 1—Saw tooth glide pattern [2]

Graver and Leonard [1, 3] developed a general dynamic model for underwater gliders based on first principles. This model was applied to examine the dynamics of gliders that traverse in a saw tooth pattern such as the Slocum [4], Spray [5] and Seaglider [6]. To investigate the dynamics of a glider in a spiral path, Bhatta [7] used perturbation theory.

Arima [8] and Isa [9] developed an underwater glider independent controllable wings. Gliders with controllable wings have a relative higher gliding performance as compared to fixed wing gliders, but have less endurance. These gliders can travel at high speeds in propeller mode, but are less efficient because of the higher drag due to the propeller. Fang Liu et al. [10] described the effect of wings geometry on the manoeuvrability of a hybrid underwater glider. Chord length has direct relation to lift-to-drag ratio of a glider. Zhang [11] investigated the wing aspect ratio of a gliding robotic fish and found that a large wing aspect ratio results in a higher gliding velocity and pitch angle [12]. In this study, the dynamic motion of a newly developed glider with a NACA 0016 rectangular and tapered wing profile is investigated. In addition, the manoeuvrability of the glider was analysed.

In Section One the dynamic model and equation of motion in the sagittal plan is presented. Section Two describes the gliders steady state spiral motion and dynamic stability. Finally the effect of pitch angle or glide angle on the glide performance is discussed.

**Dynamic Equations of Motion**

Graver [13] developed the dynamic equations of motion for a self-propelled submerged vehicle based on first principles and implemented a nonlinear controller to control its motion. In this work, the dynamics of an underwater glider with an elliptical shape with fixed wings and tail, as shown in Figure 2, is investigated. The results are generalizable, and are not glider specific. It has been modelled based on Fossen [14] equations with the hydrodynamics derivatives analytically derived based on Strip theory [15].

A glider's six degree of freedom (DOF) motion is defined in body fixed frame and inertial frame of reference. The body fixed motion components are surge, sway, heave, roll, pitch and yaw, as shown in (Fig. 2) [16-18]. The longitudinal velocity (surge) is along x- axis, lateral velocity (sway) is along y-axis and vertical speed (heave) or depth is along z-axis, with gravity positive downwards.

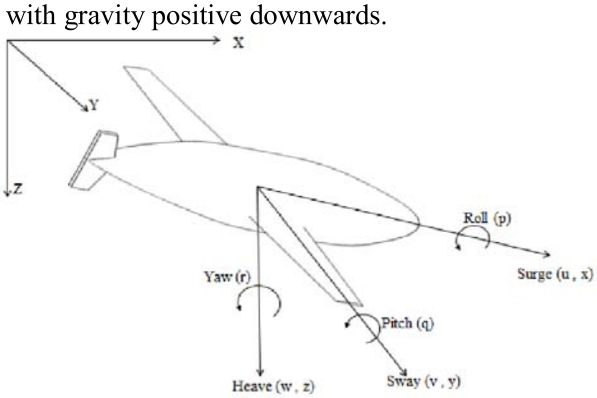


Fig. 2—Coordinates system of Glider

Assume that the position of glider in body frame of reference is denoted as $b = [x, y, z]^T$. The corresponding translational and angular velocities are represented as $v = [u, v, w]^T$ and $\omega = [p, q, r]^T$ respectively. The R matrix is used to translate the body frame of reference to the inertia fixed coordinates.

$$R = \begin{bmatrix} c\theta * c\varphi & s\varphi * s\theta * c\psi - c\varphi * s\psi & c\varphi * s\theta * c\psi + s\varphi * s\psi \\ c\theta * c\psi & c\varphi * c\psi + s\varphi * s\theta * s\psi & -s\varphi * c\psi + c\varphi * s\theta * s\psi \\ -s\theta & s\varphi * c\theta & c\varphi * c\theta \end{bmatrix}$$

where's' is sine and 'c' is cosine. $[\theta, \varphi, \psi]$ represents the pitch angle, roll angle and yaw angle respectively. The kinematic relationships are given in Equation 1-2.

$$\dot{R} = R\omega_b \quad (1)$$

$$\dot{b} = Rv_b \quad (2)$$

The generalized equation of motion of rigid body can be written as

$$M\dot{V} + C(v)v + D(v)v + g(\eta) = \tau$$

Where M is represents the mass inertia matrix of the rigid body, which includes both the rigid body and the added masses terms. C(v) denotes the matrix of centrifugal and Coriolis forces, which includes both the rigid body and the added mass terms. D(v) represents the hydrodynamic damping and lift force and g(η) is a vector representing the restoring forces and moments due to gravity and buoyancy.

Based on Fossen's work [14], the equations of motion for a rigid body in six degree of freedom are as follows

$$X = m\left[\dot{u} - vr + wq - x_g(q^2 + r^2) + y_g(pq - \dot{r}) + z_g(pr - \dot{q})\right] ...(3)$$

$$Y = m\left[\dot{v} - wp + ur - y_g(r^2 + p^2) + z_g(qr - \dot{p}) + x_g(qp + \dot{r})\right] ...(4)$$

$$Z = m\left[\dot{w} - uq + vp - z_g(p^2 + q^2) + x_g(rp - \dot{q}) + y_g(rq - \dot{p})\right] ...(5)$$

$$L = I_{xx}\dot{p} + (I_{zz} - I_{yy})qr - (\dot{r} + pq)I_{xz} + (r^2 - q^2)I_{yz} + (pr - \dot{q})I_{xy} + m[y_g(\dot{w} - uq + vp) - z_g(\dot{v} - wp + ur)] ...(6)$$

$$M = I_{yy}\dot{q} + (I_{xx} - I_{zz})rp - (\dot{p} + qr)I_{xy} + (p^2 - r^2)I_{xz} + (qp - \dot{r})I_{yz} + m[z_g(\dot{u} - vr + wq) - x_g(\dot{w} - uq + vp)] ...(7)$$

$$N = I_{zz}\dot{r} + (I_{yy} - I_{xx})pq - (\dot{q} + rp)I_{yz} + (q^2 - p^2)I_{xy} + (rq - \dot{p})I_{xz} + m[x_g(\dot{v} - wp + ur) - y_g(\dot{u} - vr + wq)] ...(8)$$

Where $[X, Y, Z]$ and $[L, M, N]$ are the external forces and moments respectively. The external forces are

$$\sum F_{ext} = F_{hydrostatic} + F_{hydrodynamic} + F_{control}$$

$$\sum M_{ext} = M_{hydrostatic} + M_{moments} + M_{control}$$

**Hydrostatic Forces and Moments**

The hydrostatic forces, including gravitational and restoring forces and moments, are

$$\begin{bmatrix} X_{Hs} \\ Y_{Hs} \\ Z_{Hs} \\ L_{Hs} \\ M_{Hs} \\ N_{Hs} \end{bmatrix} = \begin{bmatrix} (W-B)\mathrm{Sin}\theta \\ -(W-B)\mathrm{Cos}\theta * \mathrm{Sin}\varphi \\ -(W-B)\mathrm{Cos}\theta * \mathrm{Cos}\varphi \\ -(y_g W - y_b B)\mathrm{Cos}\theta * \mathrm{Cos}\varphi + (z_g W - z_b B)\mathrm{Cos}\theta * \mathrm{Sin}\varphi \\ (z_g W - z_b B)\mathrm{Sin}\theta + (x_g W - x_b B)\mathrm{Cos}\theta * \mathrm{Cos}\varphi \\ (x_g W - x_b B)\mathrm{Cos}\theta * \mathrm{Sin}\varphi + (y_g W - y_b B)\mathrm{Sin}\theta \end{bmatrix} \ldots(9)$$

Where 'W' is weight of glider and 'B' is net buoyancy force.

$W = mg$ and $B = \rho g V_{vol}$

Where m is the mass of glider, g is the gravitational forces. $\rho$ is the density of water and $V_{vol}$ the volume of the glider body. Buoyancy force is an important consideration of a glider design, whereby the glider should be neutrally buoyant (B=W). The buoyancy control system plays an important role in the glider's motion. The buoyancy mechanism has a direct relation with the lung capacity factor $\bar{\eta}$. Lung capacity factor is the percentage difference between the maximum displaced volume and the neutral buoyancy volume

$$V_{vol} = (1+\bar{\eta})V_{NB} \Leftrightarrow \bar{\eta} = \frac{V_{vol}}{V_{NB}} - 1 \ldots(10)$$

The total dry weight of the glider, W at neutral buoyancy is $W = \rho g V_{NB}$, and the net weight of glider $\overline{W}$ is

$$\overline{W} = W - B$$

$$\overline{W} = \rho g V_{NB} - \rho g(1+\eta)V_{NB}$$

$$\overline{W} = -\rho g \eta V_{NB} = -\frac{\eta}{1+\bar{\eta}}\rho g V_{vol} \ldots(11)$$

**Longitudinal Hydrodynamics Forces and Moments**

The hydrodynamic forces and moments of glider are represented by X, Y, Z, L, M and N along the body axis x, y, and z respectively. These forces and moments components are the function of linear velocities [u, v, w] and moments [p, q, r] respectively at steady state equilibrium condition. The related equations are as follows

$$\begin{bmatrix} X \\ Y \\ Z \\ L \\ M \\ N \end{bmatrix} = \begin{bmatrix} X_u & X_v & X_w & X_p & X_q & X_r \\ Y_u & Y_v & Y_w & Y_p & Y_q & Y_r \\ Z_u & Z_v & Z_w & Z_p & Z_q & Z_r \\ L_u & L_v & L_w & L_p & L_q & L_r \\ M_u & M_v & M_w & M_p & M_q & M_r \\ N_u & N_v & N_w & N_p & N_q & N_r \end{bmatrix} \begin{bmatrix} u \\ v \\ w \\ p \\ q \\ r \end{bmatrix} \ldots(12)$$

The dynamic model is simplified along the x-z plane symmetrically, so all unrelated variables $[v, p, r]$ will be zero. Also the effect of pitch rate over the drag components of glider is neglected. The unnecessary lift forces components are neglected as well during constant forward speed. Thus, the hydrodynamic forces and moments along the longitudinal plane are

$$X = X_0 + X_u u$$

$$Z = Z_0 + Z_w w + Z_q q$$

$$M = M_0 + M_w w + M_q q$$

**Equation of Motion for Glider**

The glider equations of motion along the longitudinal plane are simplified by setting all unrelated components $[v, p, r]$ to zero.

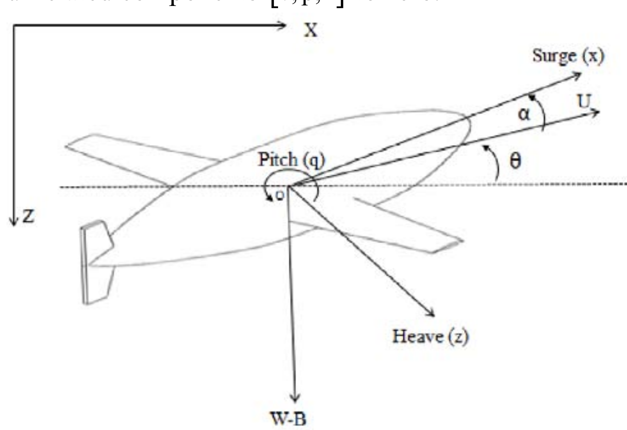


Fig. 3—Vertical Motion Coordinates of Glider

The equations, after linearization and neglecting higher order values, are

$$m[\dot{u} + z_g \dot{q}] = X_u u - [(W-B)\cos\theta]\theta_e \ldots(13)$$

$$m[\dot{w} - x_g \dot{q}] = Z_w w + Z_q q - [(W-B)\sin\theta]\theta_e + Z_{\delta t}\delta_s \ldots(14)$$

$$I_{yy}\dot{q} + m[z_g \dot{u} - x_g \dot{w}] = M_w w + M_q q - [z_g(W)\cos\theta]\theta_e + M_{\delta t}\delta_s \ldots(15)$$

These equations are expressed in matrix form below

$$M\dot{x} = C_d x + Du \quad ...(16)$$

$$M = \begin{bmatrix} m & 0 & mz_g & 0 \\ 0 & m & -mx_g & 0 \\ mz_g & -mx_g & I_{yy} & 0 \\ 0 & 0 & 0 & 1 \end{bmatrix}$$

$$C_d = \begin{bmatrix} X_u & 0 & 0 & -(W-B)\cos\theta \\ 0 & X_w & X_q & -(W-B)\sin\theta \\ 0 & M_w & M_q & -WZ_g\cos\theta \\ 0 & 0 & 1 & 0 \end{bmatrix} \quad D = \begin{bmatrix} 0 \\ Z_{\delta t} \\ M_{\delta t} \\ 0 \end{bmatrix}$$

Assumed state vector is

$$x = [u \quad w \quad q \quad \theta_e]^T$$

Given input values

$$u = [\delta_s]^T$$

Rewrite the equation 16

$$\dot{x} = M^{-1}C_d x + M^{-1}Du$$

Or

$$\dot{x} = Ax + Bu$$

The stability derivatives are calculated as follows:

$$X_u \approx -\rho v S_H C_{DH}$$

$$X_w \approx -\frac{1}{2}\rho v(S_H(C_{L\alpha\alpha} + C_{D0H}) + S_w(2C_{L\alpha\alpha}))$$

$$Z_q \approx -\rho v S_w C_{Lw} x_w$$

$$M_w \approx -\rho v S_w C_{Lw} x_w$$

$$M_q \approx -\rho v S_w C_{Lw} x_w^2$$

## Spiral Turning Motion

The spiral turning motion of an underwater glider is highly complex and nonlinear. The spiral turning motion is determined by combining the steady state turning movement and steady state gliding vector motion along the horizontal plane.

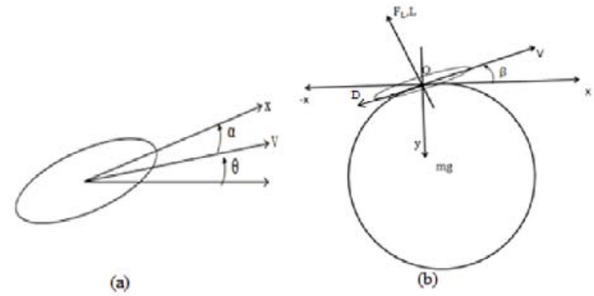


Fig. 4—Spiral motion (a) Front view (b) Top view

(Fig. 4) shows the centripetal force, $F_L$, turning radius, R and velocity, V. The relationship between turning motion and centripetal force, turning radius and velocity is as follows:

$$F_L = \frac{mV^2}{R} \quad ...(17)$$

Based on Figure 4, the following equations can be obtained:

$$D\cos\beta + L\sin\beta = 0$$

$$-D\sin\beta + L\cos\beta = F_L = \frac{mV^2}{R} \quad ...(18)$$

Where D & L are the hydrodynamic forces, β is drift angle, and m is the mass of glider.

Let's assume the drift angle is very small. Then the equation is

$$L = \frac{mV^2}{R} \quad \text{Or} \quad R = \frac{mV^2}{L} \quad ...(19)$$

The spiral glider motion is illustrated in (Fig. 5) under the influence of roll angle.

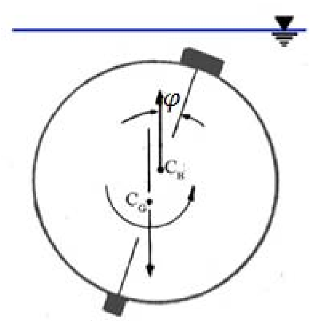


Fig. 5—Roll angle of Steady Turning Motion [19]

For stability, the metacentric height of marine vehicles is more important than the roll angle. It is the distance between the centre of gravity and centre of buoyancy. The stability of submerged vehicles depends on the distance between the centre of gravity, $C_G$ and buoyancy, $C_B$. If the distance is large, the vehicle is more stable but requires more power to maintain the pitch or roll moments of vehicle. The turning radius of spiral motion is a function of roll angle, when the roll angle is increased, the turning radius decrease vice versa [20].

**Dynamic Stability**

The hydrodynamic shape of a glider is constrained to one that provides path stability and turning performance while maintaining glide path.

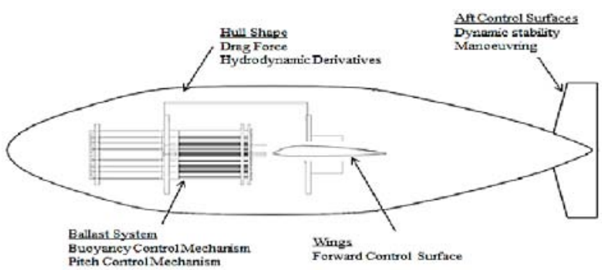


Fig. 6—Key components of the newly developed Autonomous Underwater Glider

Fig. 6 shows the key components of a newly developed glider and its hydrodynamic design.

Vertical and horizontal stability is important to ensure safe glide motion. The different levels of stability are illustrated in Fig. 7.

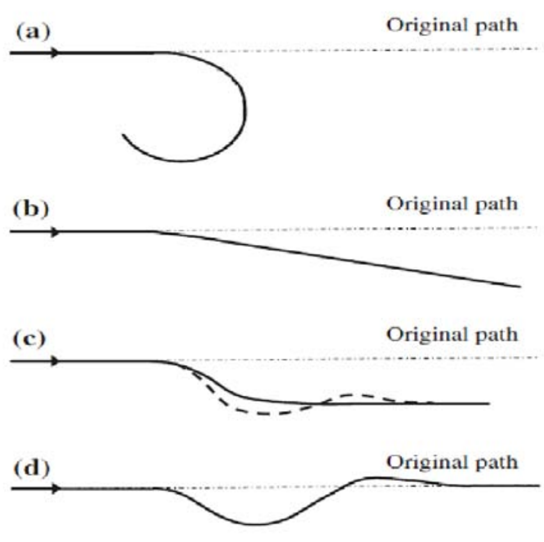


Fig. 7—Stability modes [19]

Fig. 7(a) shows an unstable motion of a glider, (b) stability along straight line shift in heading from the initial heading due to disturbance, (c) glider remains on initial heading but different path after a disturbance and (d) glider remains on original path after a disturbance.

Burcher at el [19] linearized the dynamic equation of motion along the horizontal plane.

$$(m - y_{\dot{v}})\dot{v} = y_v v + (y_v - mv)r \quad ...(20)$$

$$(I_{zz} - N_{\dot{r}})\dot{r} = N_v v + y_r r \quad ...(21)$$

The high level of manoeuvring of a glider requires dynamic stabilities in both horizontal and vertical directions. A stable glider without any control input may have straight line stability in horizontal plane. However, the hydrostatic restoring forces and moments can destabilize the glider in the vertical plane. The stability of a glider is controlled by a moving internal mass or centre of buoyancy. Alternatively, the dynamic stability of glider may be controlled by external fixed wings and a vertical rudder. The Routh stability criteria for dynamic stability in sway and yaw is

$$N_r y_v - N_v(y_r - mv) > 0$$

$$\frac{N_r}{(y_r - mv)} - \frac{N_v}{y_v} > 0 \quad ...(22)$$

In Equation 22, the first term represents the moment force and second term represents the ratio of force in vertical plane. The moment of a dynamic body must be greater than the linear velocity for a stable glider. The horizontal and vertical stability, $G_H$ and $G_V$ are given by

$$G_H = 1 - \frac{N_v(y_r - mv)}{N_r y_v} \quad ...(23)$$

$$G_V = 1 - \frac{M_w(Z_q - mv)}{M_q Z_w} \quad ...(24)$$

A non-zero dynamic stability margin indicates the unstable motion [21].

**Motion Simulation**

The dimension of a glider is defined in terms of centre of gravity and buoyancy, inertia forces, moments and volume of glider. In this study, an underwater glider is designed with an elliptical shape of 1.04 m length, 0.28 m diameter and 0.98 m wing span. The weight of the glider is 40 kg with a steady forward speed of 0.3 m/sec. The major parameters for the mathematical model are the centre of gravity and buoyancy, wetted surface area, position of moment and inertia.

After these parameters are defined, the six-degree-freedom equation of motions were used and linearized based on given assumptions and conditions. The hydrostatic forces and moments were simplified and the hydrodynamic derivatives calculated. The state space model of glider at longitudinal plane is solved using Matlab Simulink.

A linear-quadratic regulator (LQR) was used for control and the nonlinear longitudinal equation of motion was linearized. The complete linearized model in state space has four states and control inputs. The MIMO system stability is accounted for by implementation of LQR in state space representation. The LQR cost function is define as

$$J_{LQR}(u) = \int_0^\infty (x(t)^T Qx(t) + \rho u(t)^T Ru(t))dt \ldots(25)$$

Where ‘Q’ and ‘R’ are the state variable weightage matrices or positive define symmetric matrices. $\rho$ is a positive constant. The state feedback gain ‘k’ is used to design the LQR controller. ‘k’ matrix is calculated using Matlab to solve the state-space matrices A, B, Q and R.

$$x(t) = -ku(t)$$

‘Q’ and ‘R’ were selected to confirm the dynamic behaviour and motion. In this study, the ‘Q’ and ‘R’ values are

$$Q = \text{diag}[1,1,1,1]$$

$$R = \text{diag}[1]$$

$$k_{RW} = [0.1166 \quad -0.0042 \quad 0.0080 \quad 0.0276]$$

and

$$k_{TW} = [0.1496 \quad -0.0034 \quad 0.0075 \quad 0.0275]$$

Here, $k_{RW}$ and $k_{TW}$ are the gain matrices for the rectangular and tapered winged glider respectively.

**Results and Discussions**

The newly developed glider with similar span rectangular and tapered wings is shown in Fig. 8.

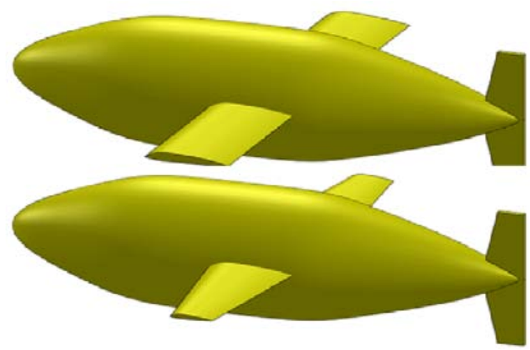

Fig. 8—Newly developed Autonomous Underwater Gliders

Two types of simulations were conducted, open loop and close loop. The numerical simulation was performed using Matlab and Simulink.

Fig. 9 and 10 shows the open loop and close loop surge velocity of the glider. The surge velocity of a tapered wing glider is 17% more compared with a glider with rectangular wings. The speed of glider has a direct relation with the surface area of the wings. The tapered wing has less surface area for a given wing span which creates less drag force as compared to the rectangular wings. However, the rectangular wings have a greater lift force because lift force is proportional to the wing area of the glider

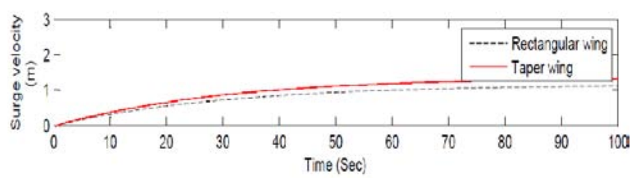


Fig. 9—Open-loop surge velocity of glider

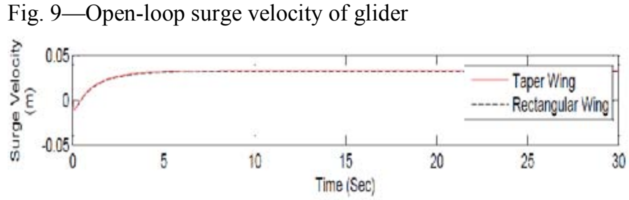


Fig. 10— Close-loop surge velocity of glider

The heave velocity of the glider with tapered wings is 15% higher, as can be seen in Fig. 11 and 12. The glider velocity is also a function of drag force. A tapered wing glider has less wetted area which generates less drag force compared to the rectangular wings. This low drag force will improve the high speed manoeuvrability of the glider.

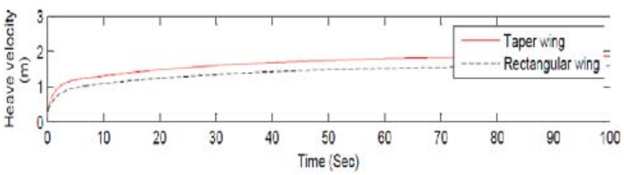


Fig.11—Open-loop heave velocity of glider

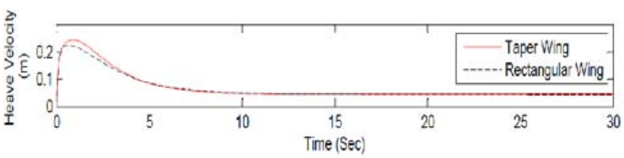


Fig. 12—Close-loop heave velocity of glider

Pitch moment is an important factor to define the stable trajectory of a glider. The pitch moment of a glider with rectangular wings is significantly higher compared to that with tapered wings, as shown in Fig. 13 and 14. This shows that, for a given aspect ratio, a glider with rectangular wings will be more stable.

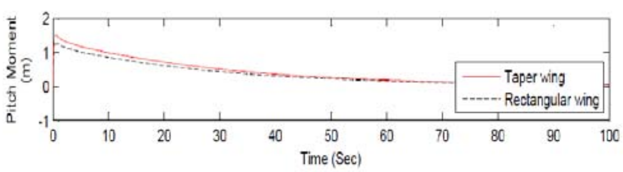


Fig. 13—Open-loop pitch moment of glider

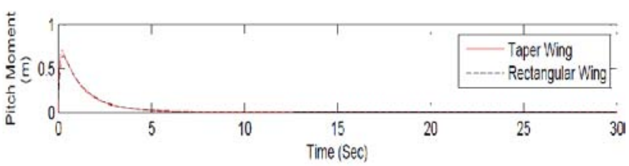


Fig. 14—Close-loop pitch moment of glider

The pitch angle or glide angle depends on the external shape of the glider. It is important to define the operational task of glider i.e. either shallow water or deep water. The speed of a glider is direct proportional to the pitch angle and is a function of the net buoyancy, which may be kept constant by changing the total volume of glider.

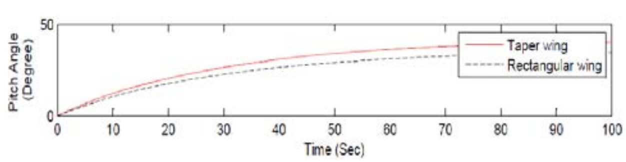


Fig. 15—Open-loop pitch angle of glider

Fig. 15 shows that the tapered wing glider has a 14% steeper pitch angle. The pitch angle of glider is directly analogous to the hydrodynamic coefficients, which based on the total wetted area of the wings.

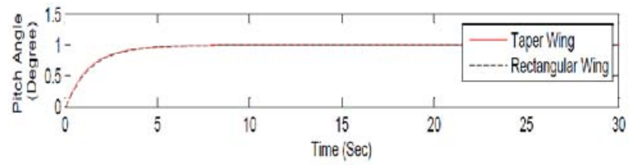


Fig. 16—Close-loop pitch angle of glider

A steep pitch angle is suitable for deep water exploration while the low pitch angle glider is design for shallow water applications i.e. XRAY glider [22, 23].

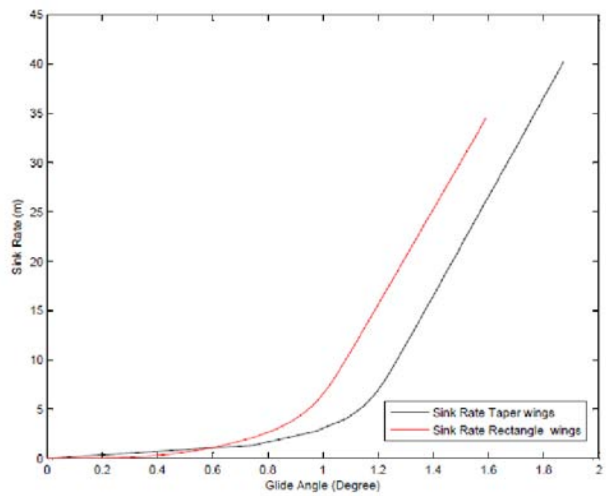


Fig. 17—Sink rate vs glide angle

Fig. 18 shows the horizontal range and sink rate of a tapered wing glider is 15% more as compare to a rectangular wing glider under the same initial conditions. The total kinetic energy (K.E) of a glider is directly analogous to the total drag force and range of glider. The relationship of operational range of glider and K.E is given as

$$D \times R_{range} = \frac{1}{2} mv^2$$

Where D is the drag force and $R_{range}$ the range of glider, v is the velocity of glider and m the total glider mass. The mass of glider is function of glider lift force is

$$L = W = mg$$

$$R_{range} = \frac{L}{D} \frac{v^2}{2g}$$

Rectangular wings have a greater wetted area, which produces more lift force, decreasing the range of the glider.

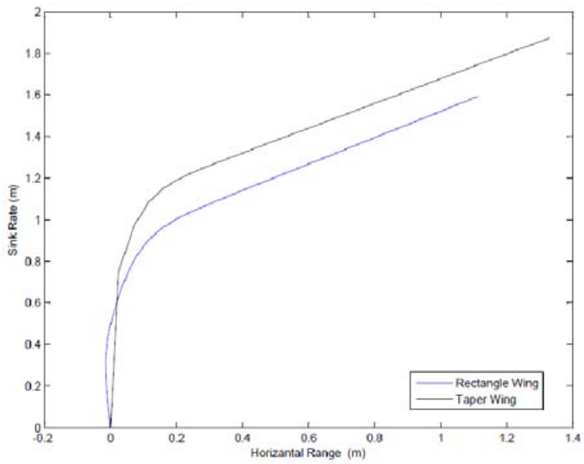


Fig. 18—Sink rate vs horizontal range

The maneuverabiliy of glider is defined by the sprial turning radius R. The radius of steady state sprial motion is a function of lift force, as given in Equation 19.

$$R = \frac{mV^2}{L}$$

Where L is the lift force of the glider, calculated using CFD [12, 24]. The lift force is perpendicular to the surge velocity of glider and has linear relation to glide angle [25, 26].

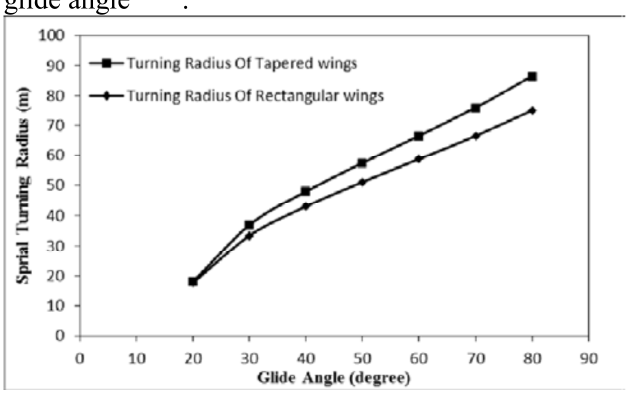


Fig. 19—Spiral motion of glider

Fig. 19 shows that the rectangular winged glider's spiral motion turning radius is less compared to tapered wing glider for a constant glide angle. Rectangular wings have high manoeuvrability because of its higher lift force. As wings play an important role in controlling the roll moments of glider during the spiral gliding motion, the rectangular wings have a more stable roll moment because of its large wetted area.

## Conclusion

The dynamic motion characteristics of a newly developed underwater glider have been investigated. The simulation results have shown that the external control surface i.e. wings, influence the linear velocity and steady turning radius of the glider. In this study, both rectangular and tapered winged gliders were investigated. A tapered wing glider has 17% higher linear velocity compared to a rectangular winged glider. However, the rectangular winged glider has more dynamic stability because of a higher pitch moment. Additionally, a rectangular winged glider has a smaller spiral turning radius i.e. better manoeuvrability. The results presented here are based on simulation and should be validated experimentally.

## Acknowledgements

Authors are thankful to Universiti Teknologi PETRONAS for providing the resources required for this work.

## Reference

1. Leonard, N. E., Graver, J. G., Model-based feedback control of autonomous underwater gliders. *IEEE J. Ocean. Eng.* 2001, 26, (4), 633-645.

2. Zhang, F., Modeling, design and control of gliding robotic fish. Michigan State University, 2014.

3. Graver, J., Liu, J., Woolsey, C., Leonard, N. E. In *Design and analysis of an underwater vehicle for controlled gliding*, Proc. 32nd Conference on Information Sciences and Systems, 1998; 1998; pp 801-806.

4. Webb, D. C., Simonetti, P. J., Jones, C. P., SLOCUM: An underwater glider propelled by environmental energy. *IEEE J. Ocean. Eng.* 2001, 26, (4), 447-452.

5. Sherman, J., Davis, R., Owens, W., Valdes, J., The autonomous underwater glider" Spray". *IEEE J. Ocean. Eng.* 2001, 26, (4), 437-446.

6. Eriksen, C. C., Osse, T. J., Light, R. D., Wen, T., Lehman, T. W., Sabin, P. L., Ballard, J. W., Chiodi, A. M., Seaglider: A long-range autonomous underwater vehicle for oceanographic research. *IEEE J. Ocean. Eng.* 2001, 26, (4), 424-436.

7. Bhatta, P., Leonard, N. E., Nonlinear gliding stability and control for vehicles with hydrodynamic forcing. *Automatica* 2008, 44, (5), 1240-1250.

8. Arima, M., Ichihashi, N., Miwa, Y. In *Modelling and motion simulation of an underwater glider with independently controllable main wings*, OCEANS 2009-EUROPE, 2009; IEEE: 2009; pp 1-6.

9. Isa, K., Arshad, M. R. In *Motion Simulation for propeller-driven USM underwater glider with controllable wings and rudder*, Instrumentation Control and Automation (ICA), 2011 2nd International Conference on, 2011; IEEE: 2011; pp 316-321.

10. Liu, F., Wang, Y., Niu, W., Ma, Z., Liu, Y. In *Hydrodynamic performance analysis and experiments of a*

*hybrid underwater glider with different layout of wings*, OCEANS 2014-TAIPEI, 2014; IEEE: 2014; pp 1-5.
11. Zhang, F., Thon, J., Thon, C., Tan, X., Miniature Underwater Glider: Design and Experimental Results. 2014.
12. Javaid Muhammad Yasar, O. M., T. Nagarajan, Syed Saad Azhar Ali, Ullah Barkat, Study on Wing Aspect Ratio on the Performance of a Gliding Robotic Fish. *Applied Mechanics and Materials* 2015, 789(2015), (978-3-03835-549-6), 248-253.
13. Graver, J. G., Underwater gliders: Dynamics, control and design. Citeseer, 2005.
14. Fossen, T. I., *Handbook of marine craft hydrodynamics and motion control*. (John Wiley & Sons, 2011.
15. Prestero, T. T. J., Verification of a six-degree of freedom simulation model for the REMUS autonomous underwater vehicle. Massachusetts institute of technology, 2001.
16. Lapierre, L., Soetanto, D., Nonlinear path-following control of an AUV. *Ocean Engineering* 2007, 34, (11), 1734-1744.
17. Lapierre, L., Soetanto, D., Pascoal, A. In *Nonlinear path following with applications to the control of autonomous underwater vehicles*, Decision and Control, 2003. Proceedings. 42nd IEEE Conference on, 2003; IEEE: 2003; pp 1256-1261.
18. Repoulias, F., Papadopoulos, E., Planar trajectory planning and tracking control design for underactuated AUVs. *Ocean Engineering* 2007, 34, (11–12), 1650-1667.
19. Burcher, R., Rydill, L. J., *Concepts in submarine design*. (Cambridge University Press, 1995; Vol. 2.
20. Su, D. H., Zhang, Y., Shi, Y., Yang, K. In *Research on Driving Mechanism and Movement Principle of Underwater Glider*, Advanced Materials Research, 2012; Trans Tech Publ: 2012; pp 6825-6831.
21. Phillips, A. B., Simulations of a self propelled autonomous underwater vehicle. University of Southampton, 2010.
22. Grund, M., Freitag, L., Preisig, J., Ball, K. In *The PLUSNet underwater communications system: acoustic telemetry for undersea surveillance*, OCEANS 2006, 2006; IEEE: 2006; pp 1-5.
23. Javaid, M. Y., Ovinis, M., Nagarajan, T., Hashim, F. B. In *Underwater Gliders: A Review*, MATEC Web of Conferences, 2014; EDP Sciences: 2014; p 02020.
24. Fujii, K., Progress and future prospects of CFD in aerospace—Wind tunnel and beyond. *PROG AEROSP SCI* 2005, 41, (6), 455-470.
25. Geisbert, J. S., Hydrodynamic modeling for autonomous underwater vehicles using computational and semi-empirical methods. Virginia Polytechnic Institute and State University, 2007.
26. Phillips, A., Furlong, M., Turnock, S. R., The use of computational fluid dynamics to determine the dynamic stability of an autonomous underwater vehicle. *P I MECH ENG* 2007, 224, (4), 239-254.